Article

Discovery Medicine 2026; 38(212): 3036–3050
https://doi.org/10.24976/Discov.Med.202638212.234

TLR3 Overexpression Attenuates D-GalN/LPS-Induced Acute Liver Injury and Is Associated With AMPK Phosphorylation, Autophagy-Related Changes, and IRF3 Upregulation

Yi Zhang[1,*], Jun Zou[1], Xiang Chen[1]

[1]Department of Critical Care Medicine, Chengdu Fifth People's Hospital, 611130 Chengdu, Sichuan, China
*Correspondence: zhangyi_cdhos5@163.com (Yi Zhang)
Submitted: 13 April 2026 Revised: 4 August 2026 Accepted: 14 August 2026 Published: 23 September 2026

Background: Toll-like receptor 3 (TLR3) has been implicated in innate immune regulation, but its role in acute liver injury is unknown. The aim of this study was to investigate the functional significance of TLR3 and its underlying mechanisms in D-GalN/lipopolysaccharide (LPS)-induced acute liver injury.

Methods: Acute liver injury models were established in rats; Kupffer cells were used to investigate the underlying cellular and molecular mechanisms. Liver function indicators, including alanine transaminase (ALT), aspartate transaminase (AST), lactate dehydrogenase (LDH), and histopathological changes in liver tissues were evaluated in rats. The expression levels of the inflammatory cytokines interleukin-1β (IL-1β) and interleukin-18 (IL-18) in Kupffer cells were measured. In addition, apoptosis was assessed in both models. To investigate the underlying molecular mechanisms, the expression of apoptosis-related proteins (B-cell lymphoma 2 (Bcl-2), Bcl-2-associated X protein (Bax)), autophagy-related markers (microtubule-associated protein 1 light chain 3 (LC3I/II), sequestosome 1 (P62)), and signaling proteins involved in the adenosine monophosphate-activated protein kinase (AMPK) and interferon regulatory factor 3 (IRF3) pathways were assessed by western blotting in both models. TLR3-overexpressing lentivirus was used to examine the functional role of TLR3. Compound C and 3-methyladenine (3-MA) were applied to inhibit AMPK signaling and autophagy, respectively. Furthermore, in Kupffer cells, the mRNA levels of IL-1β and IL-6 were detected by quantitative reverse transcription polymerase chain reaction (qRT-PCR), and autophagy was evaluated by immunofluorescence.

Results: TLR3 overexpression significantly alleviated acute liver injury and apoptosis in GalN/LPS-induced acute liver injury models. It modulated apoptosis-related proteins, enhanced autophagy markers, and was associated with increased AMPK phosphorylation and elevated IRF3 expression in both *in vivo* and *in vitro* experiments. TLR3 also lowered inflammatory cytokine expression. Notably, the protective effects of TLR3 were markedly reversed by Compound C or 3-methyladenine treatment.

Conclusion: TLR3 overexpression correlates with protection against acute liver injury, accompanied by enhanced AMPK-associated autophagy and IRF3 upregulation. These findings suggest that TLR3 links innate immune sensing with metabolic and autophagic pathways, providing a mechanistic basis for its potential protective role in acute liver injury.

Keywords: TLR3; acute liver injury; autophagy; adenosine 5-monophosphate-activated protein kinase; interferon regulatory factor 3; Kupffer cells; inflammation; apoptosis

Introduction

Liver failure (LF) is a severe form of liver injury associated with high short-term mortality and poor prognosis [1]. Common causes of LF include viral infections, drugs, and alcohol [2]. Despite advances in clinical management, LF remains an intractable disease and is frequently accompanied by complications such as spontaneous bacterial peritonitis, ascites, cirrhosis, and hepatic encephalopathy [3]. Although current therapies have improved patient outcomes, mortality remains high [4]. Treatment options mainly include pharmacological therapy and liver transplantation [5]. However, the benefit of liver transplantation are limited by donor shortages and immune-related complications [6]. Therefore, identifying effective alternative therapeutic strategies for LF is urgently needed.

The role of autophagy in LF has attracted increasing attention in recent years. Autophagy is a conserved cellular process that degrades damaged organelles and removes harmful cytosolic components [7]. In particular, microtubule-associated protein 1 light chain 3 (LC3) is closely associated with phagocytosis [8]. Autophagy has been shown to protect against acetaminophen-induced liver injury [9]. Moreover, reduced liver cell autophagy promotes interleukin (IL)-1β/tumor necrosis factor (TNF)-

induced cell necrosis in mice [10]. Therefore, modulation of autophagy may represent a potential therapeutic strategy for LF.

Moreover, autophagy is one of the key metabolic processes regulated by adenosine 5-monophosphate-activated protein kinase (AMPK) [11,12]. AMPK plays an important role in various forms of liver injury. For example, AMPK protects against alcohol-induced liver injury by promoting ubiquinolcytochrome c reductase core protein 2 (UQCRC2)-mediated mitophagy [13]. Hyperglycemia aggravates thioacetamide-induced acute liver injury by inhibiting AMPK/mammalian target of rapamycin (mTOR)-mediated autophagy in liver-resident macrophages [14]. In addition, dexmedetomidine alleviates sepsis-induced liver injury by promoting autophagy and activating the AMPK signaling pathway [15]. Therefore, modulation of autophagy and AMPK signaling may represent a potential therapeutic strategy for LF.

Toll-like receptor 3 (TLR3), a member of the TLR family, plays an important role in innate immunity and the regulation of immune responses [16]. A previous study has shown that TLR3 contributes to antiviral host response by regulating type I interferons (IFNs) and proinflammatory factors [17]. TLR3 expression has also been reported to decrease during acute liver injury [18]. Notably, the AMPK signaling pathway was suppressed in TLR3 knockout mice [19]. Viral infection can activate AMPK signaling and enhance the interaction between receptor for activated C kinase 1 (RACK1) and interferon regulatory factor 3 (IRF3) [20]. In addition, reduced TLR3 activity has been associated with impaired autophagy in acute pancreatitis [21], whereas TLR3 activation enhances autophagy in mouse models of heart failure [22]. Selective autophagy can also regulate IRF3 stability, thereby modulating IFN production and immune function [23]. Therefore, this study aims to investigate the relationships among TLR3 overexpression, autophagy, AMPK phosphorylation, and IRF3 expression in GalN/LPS-induced acute liver injury

Materials and Methods

Animals Statement

Beijing Vital River Laboratory Animal Technology Inc. (102; Beijing, China) provided the wistar rats. Fifty-three male rats (7–8 weeks old, 276–300 g) were housed at room temperature (20–25 °C) and 55–65% humidity under a 12-hour light-dark cycle. Standard food and water were available ad libitum. All rat experiments were approved by the Institutional Animal Care and Use Committee of the Zhejiang Center of Laboratory Animals (Approval No. ZJCLA-IACUC-20011191) and were conducted in accordance with the guidelines of the China Council on Animal Care and Use.

Establishment of a Rat Model of Acute Liver Injury

Lentivirus Packaging and Purification

Lentiviral particles were generated by co-transfecting 293T cells with three plasmids: the transfer plasmid (LV-TLR3 or LV-NC), the packaging plasmid psPAX2 (Addgene #12260, Watertown, MA, USA), and the envelope plasmid pMD2.G (Addgene #12259, Watertown, MA, USA). The LV-TLR3 transfer plasmid was constructed by inserting the full-length rat TLR3 coding sequence (CDS; based on NCBI Reference Sequence NM_198791.2) into the GV341 vector (Jikai Gene, Shanghai, China; carrying a 3×Flag tag and puromycin resistance gene). The TLR3 CDS sequence is provided in **Supplementary Table 1**. Transfection was performed using Lipofectamine 3000 (L3000015, Invitrogen, Carlsbad, CA, USA) following the manufacturers protocol. Briefly, 293T cells at 70–80% confluence in 10 cm dishes were transfected with 15 µg of transfer plasmid, 10 µg of psPAX2, and 5 µg of pMD2.G, all diluted in Opti-MEM. After 6 hours, the medium was replaced with fresh DMEM containing 10% FBS. Viral supernatants were collected at 48 and 72 hours post-transfection, pooled, and centrifuged at 2000 ×g for 10 minutes to remove cell debris. The clarified supernatant was filtered through a 0.45 µm filter and concentrated by ultracentrifugation at 72,000 ×g for 2 hours at 4 °C. The viral pellet was resuspended in PBS and stored at –80 °C. Viral titers were determined by quantitative reverse transcription polymerase chain reaction (qRT-PCR) or by limiting dilution in 293T cells.

Animal Model and Treatment

After 7 days of acclimatization, forty-eight Wistar rats were used to establish an acute liver injury model. 48 Wistar rats were split into various treatment groups at random (eight rats per group): control (Con), model (Mod), LV-NC, LV-TLR3, LV-TLR3 + compound C (CC) and LV-TLR3 + 3-methyladenine (3-MA) groups. The model (Mod) group: Wistar rats were only injected with 700 mg/kg d-galactosamine (GalN; G0500; Merck, Shanghai, China) and 10 µg/kg lipopolysaccharide (LPS; 916374; Merck, Shanghai, China). The Con group: Wistar rats were intraperitoneally injected with 1 × phosphate buffer saline (PBS; P1020; Solarbio, Beijing, China) of the same amount. According to a previous study, Wistar rats in the LV-NC and LV-TLR3 groups were intraperitoneally injected with TLR3-overexpressing lentivirus (LV-TLR3; GV341 vector; 3 flag, non-fluorescence, puromycin; 5 × 10^8 pfu/100 µL; Jikai Gene, Shanghai, China) or LV-NC at 48 h before modeling [24]. The LV was packaged in 293T cells (BNCC353535; BeNa Biology, Henan, China), which were cultured in dulbecco's modified eagIe's medium (DMEM; SH30022.01B; Hyclone, UT, USA) with 10% fetal bovine serum (FBS; 10100147; Thermo Fisher Scientific, MA, USA). The LV-TLR3 + CC group: Wistar rats were injected with LV-TLR3 and CC (AMPK inhibitor,

20 mg/kg; S7840; Selleck, USA) before being treated with GalN and LPS. CC was injected into Wistar rats 1 h before modeling [25]. The LV-TLR3 + 3-MA group: Wistar rats were injected with LV-TLR3 and 3-MA (autophagy inhibitor; 30 mg/kg; S2767; Selleck, USA) before being treated with GalN and LPS. 3-MA was injected into Wistar rats 1.5 h before modeling [26]. After that, rats in LV-NC, LV-TLR3, LV-TLR3 + CC, and LV-TLR3 + 3-MA were intraperitoneally injected with GalN (700 mg/kg) and LPS (10 μg/kg) to induce LF [27,28]. Rats were anesthetized with pentobarbital sodium (80 mg/kg; JX082085, sh-jxsw, Shanghai, China) after 12 hours. Under aseptic conditions, whole venous blood was collected from the inferior vena cava. Subsequently, the Wistar rats were sacrificed by cervical dislocation, and liver tissues were harvested.

Enzyme Linked Immune Sorbent Assay (ELISA)

The activities of enzymes, including alanine transaminase (ALT), aspartate transaminase (AST), lactic dehydrogenase (LDH), as well as the levels of inflammation-related factors (IL-1β and IL-18) were assessed by ELISA assay. Rat ALT, AST, LDH, IL-1β and IL-18 ELISA kits were purchased from Feien Biology (ER0255; ER0470; ER0646; ER0036; ER1094; Wuhan, China). According to manufacturer's instructions, collected serum sample was placed at 25 °C for 2 h and then centrifuged for 20 min at 1000 ×g to obtain supernatant. The collected cell culture supernatant was centrifuged for 20 min at 1000 ×g and at 4 °C. The collected supernatant was immediately used for subsequent assays. All reagents and samples were equilibrated to room temperature before detection. The ELISA plate was washed twice with 300 μL of wash buffer. Two-fold diluted standard (100 μL) were added to the standard wells, and standard diluent (100 μL) was added to the blank well. After adding 100 μL of each sample to the wells, the plate was incubated at 37 °C for 1.5 hours. Following washing, the samples were incubated with biotin-labeled antibody working solution (100 μL per well) at 37 °C for 1 h. After washing, the samples were incubated with horseradish peroxidase conjugate working solution (100 μL per well) at 37 °C for 30 min. After another washing step, tetramethylbenzidine (TMB) substrate solution (90 μL) was added, and the plate was incubated for 20 minutes (37 °C, without light). Subsequently, 50 μL of stop solution was added to each well, and the absorbance at 450 nm was measured using a microplate reader (HTS-XT; Bruker Optics, Rheinstetten, Germany).

Hematoxylin-Eosin (HE) Staining Assay

The morphological structure of liver was detected using an HE staining kit (C0105S; Beyotime, Shanghai, China). Liver tissues were fixed in 4% paraformaldehyde (P0099, Beyotime, Shanghai, China) at 4 °C for 24 h. After fixation, the tissues were dehydrated through a graded ethanol series (70%, 80%, 90%, and 100% ethanol; 30 min each), cleared in xylene (A530011, Sangon Biotech, Shanghai, China) twice for 10 min each, and embedded in paraffin (A601888, Sangon, Shanghai, China) at 60 °C. Liver tissues were sectioned using a tissue slicer (HS-S7220-B; Shenyang Hengsong Technology, Liaoning, China) at a thickness of 5–10 μm. According to the manufacturer's guidelines, the tissue sections were dewaxed twice in xylene (A530011; Sangon Biotech, Shanghai, China) for 10 min each. After sequential treatment with graded ethanol (100%, 90%, 80% and 70%) and distilled water, the samples were stained with hematoxylin solution for 5 min. Excess staining solution was rinsed off with tap water for 10 min. After washing with distilled water, the samples were stained with eosin staining solution for 1 min and then sequentially dehydrated with graded ethanol (70%, 80%, 90 and 100%). After clearing twice in xylene for 5 min each, the samples were mounted with neutral gum (E675007; Sangon Biotech, Shanghai, China). Finally, the stained liver sections were photographed under a light microscope (magnification, ×100; LV150; Nikon Inc., Tokyo, Japan).

Terminal-Deoxynucleoitidyl Transferase Mediated Nick End Labeling (TUNEL) Staining Assay

The apoptosis of liver tissue cells was assessed using a TUNEL kit (C1098; Beyotime, Shanghai, China). Tissue sections were dewaxed in xylene for 10 min and sequentially treated with graded ethanol (100%, 90% and 70%) and distilled water. The sections were incubated with Proteinase K (20 μg/mL; ST532; Beyotime, Shanghai, China) at 37 °C for 30 min. After washing, the tissue sections were incubated with peroxidase blocking buffer (P0100B; Beyotime, Shanghai, China) at 37 °C for 20 min. Subsequently, biotin labeling solution (5 μL terminal deoxynucleotidyl transferase (TdT) + 45 μL Biotin-2′-deoxyuridine 5′-triphosphate (dUTP)) was added, and the sections were incubated at 37 °C for 1 h in the dark. The tissue sections were then incubated with reaction termination solution (200 μL) at 25 °C for 10 min and washed before subsequent procedure. Horseradish peroxidase working solution (50 μL) was added, and the sections were incubated at 25 °C for 30 min. Subsequently, Diaminobenzidine chromogenic solution (300 μL) was applied for 20 min at 25 °C. The sections were counterstained with hematoxylin for 5 min. Images of apoptotic liver cells were captured using a light microscope (brown staining; magnification ×100). TUNEL-positive cells were counted in at least five randomly selected fields per section, and the mean number of positive cells per field was calculated for each group.

Isolation, Identification and Culture of Rat Kupffer Cells

According to a previous study [14], Kupffer cells were isolated from 5 Wistar rats (separate healthy rats obtained from the same vendor as described in the Animals Statement, and not used for the *in vivo* model experi-

ments). Prior to liver perfusion, the rats were anesthetized by intraperitoneal injection of pentobarbital sodium (80 mg/kg; JX082085, sh-jxsw, China). The liver was sequentially perfused with warmed Hanks' balanced salt solution (PB180323, procell, Wuhan, China) at 37 °C and collagenase IV (A004210; Sangon Biotech, Shanghai, China). After perfusion and collagenase digestion, the rats were deeply anesthetized and euthanized by cervical dislocation. The liver tissues were cut into pieces, digested for 30 min, and filtered through 70 µm cell strainers (352350; Corning, NY, USA) to obtain liver cell suspensions. Nonparenchymal cells were separated from the liver cell suspensions by differential centrifugation (three times, 50 ×g for 2 min). Subsequently, 50% and 25% percoll gradient solution (P8370; Solarbio, Beijing, China) were sequentially used to isolate Kupffer cells by centrifugation at 1800 ×g and 4 °C for 15 min.

For further identification of Kupffer cells, immunofluorescence staining and flow cytometry were performed using anti-rat ED1 (MCA341, Bio-Rad, Hercules, CA, USA) and ED2 antibodies (MCA342, Bio-Rad, Hercules, CA, USA). The purity of Kupffer cells was determined as the percentage of $ED1^+/ED2^+$ double-positive cells by flow cytometry, and co-localization of both markers was confirmed by immunofluorescence. For immunofluorescence staining, cells were fixed with 4% paraformaldehyde for 15 min, blocked with 5% goat serum for 1 h at 25 °C, and incubated with primary antibodies overnight at 4 °C. After washing, cells were incubated with Alexa Fluor 488-conjugated goat anti-mouse IgG (green; 1:500; Invitrogen, A-11001, Carlsbad, CA, USA) for 1 h at 25 °C in the dark. Nuclei were counterstained with DAPI. Images were captured using a confocal fluorescence microscope (TCS SP8, Leica, St. Louis, MO, USA). For flow cytometry, cells were sequentially incubated with anti-rat ED1 primary antibody, followed by Alexa Fluor 488-conjugated goat anti-mouse IgG, blocked with normal mouse serum, then incubated with anti-rat ED2 primary antibody, followed by PE-conjugated secondary antibody (M30204, Thermo Fisher, Waltham, MA, USA). Data were acquired on a flow cytometer (Attune NxT, Thermo Fisher Scientific, Waltham, MA, USA) and analyzed using FlowJo software (v10, BD Biosciences, Franklin Lakes, NJ, USA).

The collected Kupffer cells were cultured in DMEM supplemented with 10% FBS and 0.1% penicillin/streptomycin (15140122; Thermo Fisher Scientific, MA, USA) at 37 °C for 15 min. Nonadherent cells were removed by replacing the medium with fresh medium. All cell preparations tested negative for mycoplasma contamination using a mycoplasma detection kit (Beyotime, C0301S, Shanghai, China) according to the manufacturer's instructions.

Western Blot Analysis

Rat liver tissues were collected and homogenized for total protein extraction. In addition, rat Kupffer cells (5×10^5 cells/well) were seeded into 6-well plates. After 24 h, the cells were treated with different compounds for 48 h and then collected for total protein extraction. A protein extraction kit (C006225; Sangon Biotech, Shanghai, China) was used, and protein concentration were determined using a protein assay kit (P0010; Beyotime, Shanghai, China). Gel reagents (P0012A; P0690; Beyotime, Shanghai, China) were used to separate the total proteins. The proteins were then transferred onto 0.45 µm membranes (FFP32; Beyotime, Shanghai, China). After blocking with 5% skimmed milk, the membranes were sequentially incubated with primary antibodies for 2 h at 25 °C and secondary antibodies for 1 h at 25 °C. The antibodies used are listed in Table 1. Glyceraldehyde-3-phosphate dehydrogenase (GAPDH) was used as the internal reference. An electro-chemiluminescence kit (32209; Thermo Fisher Scientific, Waltham, MA, USA) was used to visualize the protein bands. Images were captures using a gel imaging analysis equipment (GeneGenius; Baijing Biotechnology Inc., Beijing, China). Band intensities were analyzed using ImageJ (Version 1.54d, NIH, Bethesda, MD, USA), normalized to GAPDH, and expressed as fold changes relative to the control group based on three independent experiments.

Establishment of a Cell Model of Acute Liver Injury and Cell Treatment

Kupffer cells were randomly divided into different treatment groups: Con, Mod, LV-NC, LV-TLR3, LV-TLR3 + CC and LV-TLR3 + 3-MA group. According to a previous study, Kupffer cells in the Mod group were treated with GalN/LPS (GalN: 1 mmol/L; LPS: 10 ng/mL) for 24 h to establish an acute liver injury model *in vitro* [24]. Cells in the Con group were cultured under normal conditions. Cells in the LV-NC, LV-TLR3 group were seeded into 6-well plates (2×10^5 cells/well). When cell confluence reached 60%, they were treated with LV at a multiplicity of infection (MOI) of 25 (5×10^6 pfu per 2×10^5 cells) [29]. Puromycin (1 µg/mL; P8230; Solarbio, Beijing, China) was used to select stably transduced cells. After 48 h of culture, the cells were treated with GalN/LPS (GalN: 1 mmol/L; LPS: 10 ng/mL) for 24 h. Kupffer cells in the LV-TLR3 + CC and LV-TLR3 + 3-MA groups were first infected with LV-TLR3. After 48 h, the cells were treated with 25 µM CC [30] or 5 mM 3-MA [29] for 2 h, followed by stimulation with GalN/LPS (GalN: 1 mmol/L; LPS: 10 ng/mL) for 24 h.

qRT-PCR

Total RNA was extracted from rat Kupffer cells using an RNA extractor kit (B511311; Sangon Biotech, Shanghai, China). RNA concentration was measured using a spectrophotometer (840-211000; Thermo Fisher Scientific,

Table 1. Antibodies used in this study.

Name	Catalog	Molecular weight	Dilution	Manufacturer
Bcl-2	ab194583	26 kDa	1/2000	abcam, UK
Bax	ab32503	21 kDa	1/5000	abcam, UK
LC3I	ab192890	16 kDa	1/2000	abcam, UK
LC3II	ab192890	14 kDa	1/2000	abcam, UK
P62	ab109012	62 kDa	1/20,000	abcam, UK
TLR3	ab137722	104 kDa	1/5000	abcam, UK
p-AMPK	ab133448	64 kDa	1/5000	abcam, UK
AMPK	ab110036	64 kDa	1/2000	abcam, UK
IRF3	ab238521	47 kDa	1/2000	abcam, UK
GAPDH	ab8245	37 kDa	1/5000	abcam, UK
Goat anti rabbit	ab97051	—	1/10,000	abcam, UK
Goat anti mouse	ab96879	—	1/10,000	abcam, UK

Bcl-2, B-cell lymphoma 2; Bax, Bcl-2-associated X protein; LC3I, microtubule-associated protein 1 light chain 3 I; LC3II, microtubule-associated protein 1 light chain 3 II; P62, sequestosome 1; TLR3, toll-like receptor 3; AMPK, adenosine 5-monophosphate-activated protein kinase; p-AMPK, phosphorylation-AMPK; IRF3, interferon regulatory factor 3; GAPDH, glyceraldehyde-3-phosphate dehydrogenase.

Table 2. The primer sequences of related genes.

Gene	Forward primer	Reverse primer
TLR3	GATTGGCAAGTTATTCGTC	GCGGAGGCTGTTGTAGG
IL-1β	GACTTCACCATGGAACCCGT	GGAGACTGCCCATTCTCGAC
IL-6	CACTTCACAAGTCGGAGGCT	TCTGACAGTGCATCATCGCT
GAPDH	ACGGGAAACCCATCACCATC	TCACAAACATGGGGGCATCA

IL-1β, interleukin-1β; IL-6, interleukin-6; GAPDH, glyceraldehyde-3-phosphate dehydrogenase.

MA, USA). cDNA was synthesized using a FastQuant RT kit (KR106-03; Tiangen Biotech, Beijing, China). The amplified cDNA was assessed using a SYBR Green kit (F-416L; Thermo Fisher Scientific, MA, USA). The cycling conditions were as follows: 95 °C for 10 min, followed by 40 cycles of 95 °C for 15 s, 60 °C for 30 s, and 72 °C for 30 s, with melting curve analysis. qRT-PCR was performed using an MJOpticon2 instrument (Bio-Rad Inc., Hercules, CA, USA). GAPDH was used as internal reference. Relative gene expression was calculated using the $2^{-\Delta\Delta ct}$ method. The primers are listed in Table 2 and were synthesized by Thermo Fisher Scientific (Waltham, MA, USA).

Flow Cytometry Assay

Rat Kupffer cells were digested with 0.25% trypsin (without ethylene diamine tetraacetic acid; C0205; Beyotime, Shanghai, China). Cell apoptosis was assessed using 5×10^5 cells per sample with an annexin V-fluorescein isothiocyanate (FITC)/propidium iodide (PI) apoptosis detection kit (40302ES60; Yeasen Biotechnology, Shanghai, China). According to the manufacturer's instructions, cells were resuspended in 100 µL of 1 × binding buffer. Annexin V-FITC (5 µL) and PI staining solution (10 µL) were added to the cell suspension and gently mixed, followed by incubation at 25 °C for 12 min in the dark. After the addition of 400 µL of 1 × binding buffer, the samples were placed on ice. Cell apoptosis was assessed using a flow cytometer (PL00285; Thermo Fisher Scientific, Waltham, MA, USA). Data were analyzed using FlowJo software (v10, BD Biosciences, Franklin Lakes, NJ, USA). The total apoptosis rate (Annexin V^+/PI^- [early] + Annexin $V^+//PI^+$ [late]) was calculated based on three independent experiments.

Immunofluorescence Assay

Rat Kupffer cells (5×10^4) were seeded onto cover glasses (WHB-6-CS, whb, Shanghai, China). After cell adhesion, the cells were fixed with 4% paraformaldehyde (P0099; Beyotime, Shanghai, China) for 15 min at 25 °C. After washing with 1 × PBS, the cells were permeabilized with Triton X-100 (P0096; Beyotime, Shanghai, China) for 10 min and then blocked with immunostaining blocking buffer (P0102; Beyotime, Shanghai, China) for 1 h. The cells were sequentially incubated with a primary antibody against LC3B (at 4 °C overnight; ab192890; 1 µg/mL; abcam, UK) and a secondary antibody (avoiding light at 25 °C for 2 h; ab150078; Alexa Fluor® 555; 1:500; abcam, UK). Antifade mounting medium containing

4,6-diamino-2-phenyl indole (DAPI) (P0131; Beyotime, Shanghai, China) was used to prevent fluorescence quenching. Finally, images were captured using a confocal fluorescent microscope (magnification ×200; TCS SP8; Leica Camera AG Inc., Solms, Wetzlar, Germany). The relative LC3B fluorescence intensity was quantified using ImageJ software (NIH, Bethesda, MD, USA) and normalized to the control group.

Statistical Analysis

Data were expressed as the mean ± standard deviation. Normality of data distribution was assessed using the Shapiro–Wilk test, and homogeneity of variance was evaluated using Levene's test. One-way analysis of variance (ANOVA) was used to compare multiple groups, followed by Tukey's honest significant difference post hoc test for pairwise comparisons. $p < 0.05$ was considered statistically significant. Statistical analyses were performed using GraphPad Prism 8.0 (Graphpad Software Inc., Boston, MA, USA).

Results

The Preventive Effect of TLR3 on Acute Liver Injury was Reversed by CC and 3-MA in Rats

To examine the role of TLR3 in GalN/LPS-induced acute liver injury, we injected TLR3-overexpressing lentivirus into rats treated with or without CC and 3-MA. qRT-PCR analyses confirmed successful TLR3 overexpression *in vivo* (**Supplementary Fig. 1A**). Compared with the Con group, serum ALT, AST and LDH levels were significantly increased in the Mod group (Fig. 1A–C, $p < 0.001$). Histopathological findings also revealed marked hepatocellular edema, cell lysis, diffuse necrosis, and inflammatory cell infiltration (Fig. 1E), confirming successful establishment of the acute liver injury model. However, compared with the LV-NC group, LV-TLR3 significantly reduced ALT, AST and LDH levels in model rats (Fig. 1A–C, $p < 0.01$). Interestingly, compared with the LV-TLR3 group, the decreases in ALT, AST and LDH were reversed by CC or 3-MA (Fig. 1A–C, $p < 0.05$). CC and 3-MA were inhibitors of AMPK and autophagy, respectively. These results revealed that TLR3 may reduce ALT, AST and LDH levels by regulating AMPK and autophagy in acute liver injury model rats. Moreover, liver cell apoptosis (brown) was also alleviated by TLR3 overexpression (Fig. 1D,F, $p < 0.001$). However, the effects of TLR3 overexpression on liver tissue lesions and cell apoptosis (brown) were reversed by CC or 3-MA (Fig. 1E,F). These results indicate that TLR3 overexpression is associated with reduced ALT, AST and LDH levels, and that AMPK and autophagy are involved in this effect.

The Regulatory Effects of TLR3 on Apoptosis-Related and Autophagy-Related Proteins, As Well As on AMPK Phosphorylation and IRF3 Expression, Were Reversed by CC and 3-MA.

To investigate the molecular mechanism of TLR3 in acute liver injury, we examined related protein expression. TLR3 overexpression significantly increased Bcl-2 expression and decreased Bax expression in acute liver injury model rats (Fig. 2A–C, $p < 0.001$). Following treating with CC or 3-MA, the effects of TLR3 overexpression on Bcl-2 and Bax proteins were reversed (Fig. 2A–C, $p < 0.05$). These results suggest that TLR3 may delay acute liver injury by regulating apoptosis-related proteins in rats, and that AMPK and autophagy may be involved in this process.

Additional findings showed that TLR3 regulated the expression of autophagy-related proteins (LC3I, LC3II, and P62) in acute liver injury model rats. Compared with the LV-NC group, LV-TLR3 increased the LC3II/LC3I ratio and decreased the expression of P62, indicating increased autophagy (Fig. 2D–F, $p < 0.001$). Moreover, compared with the Con group, TLR3 expression was significantly decreased in the Mod group (Fig. 2G,H, $p < 0.001$). Importantly, TLR3 overexpression significantly increased IRF3 expression in acute liver injury model rats (Fig. 2G,I, $p < 0.001$). In addition, compared with the LV-NC group, LV-TLR3 increased the phosphorylation-AMPK (p-AMPK)/AMPK ratio, indicating activation of the AMPK pathway in liver injury model rats (Fig. 2G,J, $p < 0.001$). In particular, the regulatory effects of TLR3 overexpression on the AMPK pathway and autophagy-related proteins were reversed by CC or 3-MA (Fig. 2D–G,I,J, $p < 0.05$). These results indicate that TLR3 overexpression is associated with AMPK phosphorylation and enhanced autophagy *in vivo*, and that pharmacological inhibition of AMPK or autophagy attenuates these TLR3-associated effects.

The Regulatory Effects of TLR3 on Inflammatory Factors, Cell Apoptosis, and Apoptosis-Related Proteins Were Reversed by CC and 3-MA in Kupffer Cells

Prior to the experiments, we identified the isolated primary rat Kupffer cells. Immunofluorescence staining and flow cytometry confirmed that the isolated cells were $ED1^{+}/ED2^{+}$ double-positive, indicating high-purity Kupffer cells (**Supplementary Fig. 2**). We also verified TLR3 overexpression in Kupffer cells after LV-TLR3 transduction. qRT-PCR analyses confirmed successful TLR3 overexpression *in vitro* (**Supplementary Fig. 1B**). In the GalN/LPS-induced acute liver injury cell model, we further investigated the effects of TLR3 on inflammatory factors, cell death, and apoptosis-related proteins. First, Kupffer cells were sequentially treated with LV, CC and 3-MA. qRT-PCR and ELISA results showed that TLR3 overexpression significantly reduced the levels of the inflamma-

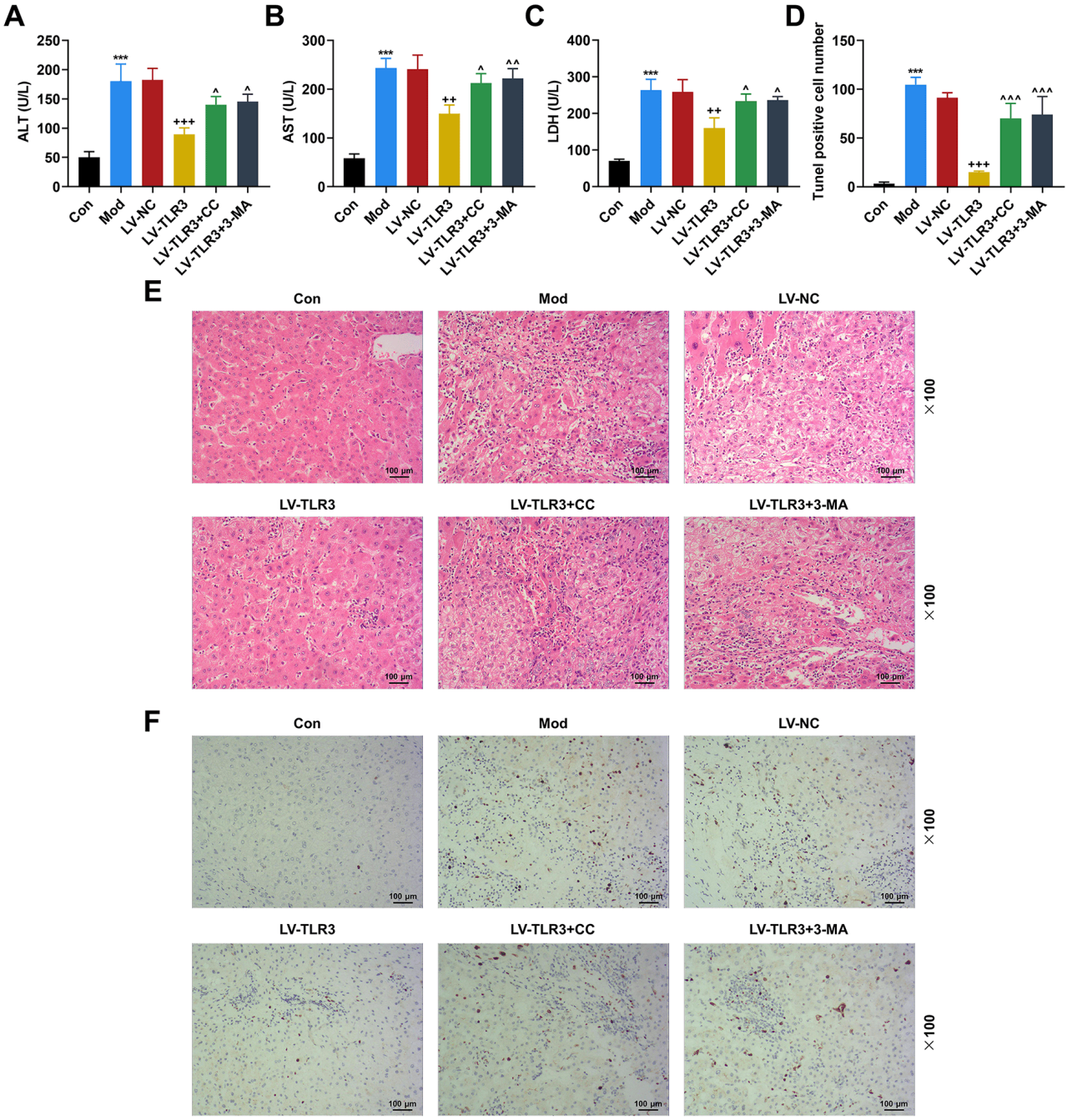

Fig. 1. The preventive effect of TLR3 on acute liver injury were reversed by CC and 3-MA. For (A–E), Rats were divided into the following groups: untreated control (Con), model (Mod, GalN/LPS only), lentivirus negative control (LV-NC), TLR3-overexpressing lentivirus (LV-TLR3), LV-TLR3 combined with Compound C (LV-TLR3 + CC), and LV-TLR3 combined with 3-methyladenine (LV-TLR3 + 3-MA) before establishing acute liver injury model. (A–C) ELISA assay was used to detect the levels of ALT, AST and LDH in rat whole blood. (E) HE staining assay was used to examine the morphological structure of rat liver tissue. Resolution: 100 μm, ×100. (F) TUNEL assay was used to detect the liver cell apoptosis in rats, and (D) presents the corresponding quantitative results. Positive staining shown in brown. Resolution: 100 μm, ×100. $^{***}p < 0.001$ vs. Con group. $^{++}p < 0.01$, $^{+++}p < 0.001$ vs. LV-NC group. $^{\wedge}p < 0.05$, $^{\wedge\wedge}p < 0.01$, $^{\wedge\wedge\wedge}p < 0.001$ vs. LV-TLR3 group. 8 rats per group, and data from each group were obtained from three repeated experiments. ALT, alanine transaminase; AST, aspartate transaminase; LDH, lactic dehydrogenase; Con, control; Mod, model; LV, lentivirus; NC, negative control; TLR3, toll-like receptor 3; CC, compound C; 3-MA, 3-methyladenine; ELISA, enzyme linked immune sorbent assay; HE, hematoxylin-eosin; TUNEL, terminal-deoxynucleoitidyl transferase mediated nick end labeling. Note for Fig. 1E: The vacuole-like structures visible in the control group are normal central veins, a physiological feature of liver tissues.

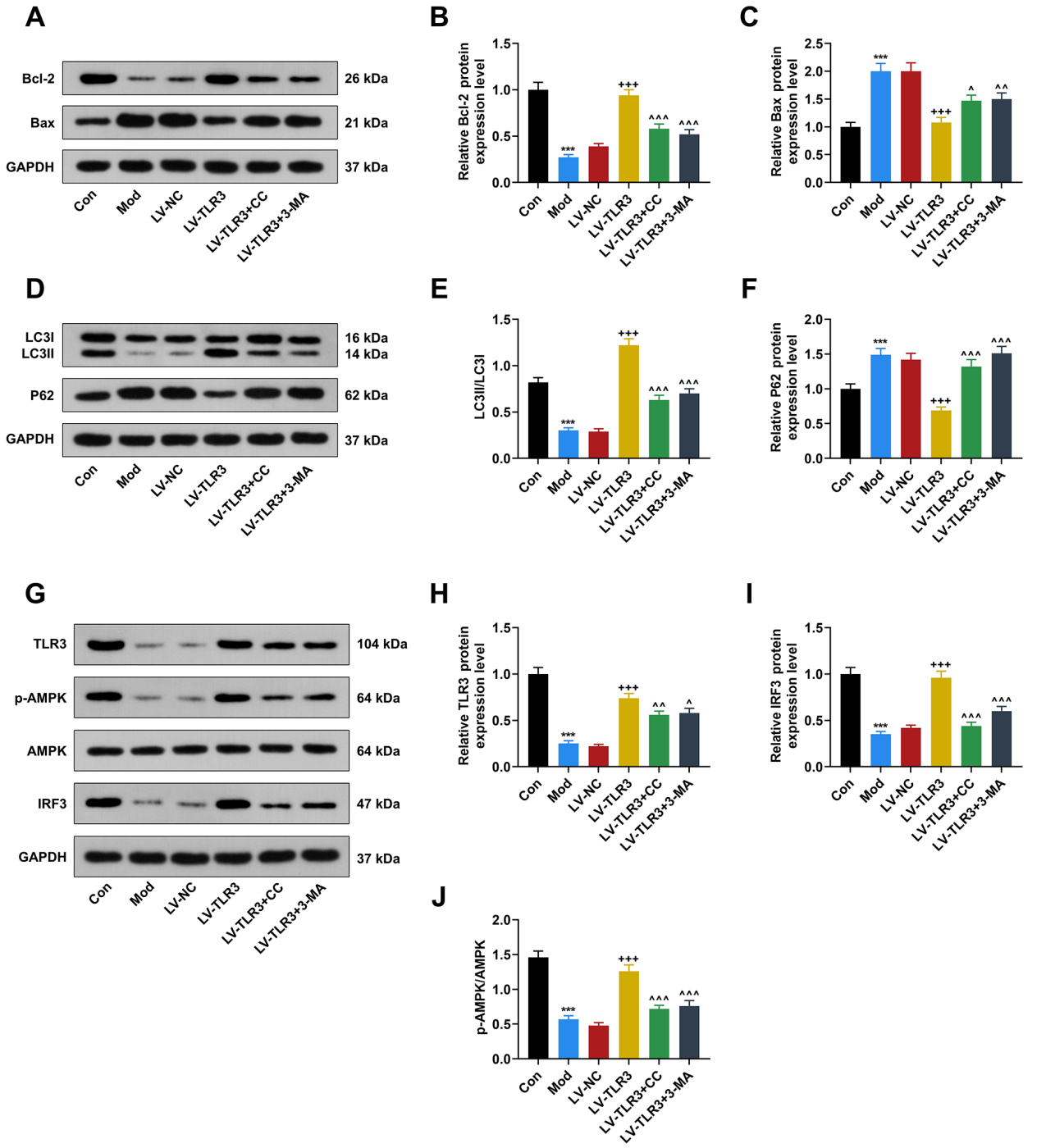

Fig. 2. The regulatory effects of TLR3 on apoptosis-related and autophagy-related proteins, p-AMPK, AMPK and IRF3 were reversed by CC and 3-MA. For (A–J) Rats were pretreated with Con, Mod, LV-NC, LV-TLR3, LV-TLR3 + CC, or LV-TLR3 + 3-MAbefore establishing acute liver injury model. (A–J) Protein expression levels of Bcl-2, Bax, LC3I, LC3II, P62, TLR3, p-AMPK, AMPK, IRF3 and GAPDH were detected by western blot assay in rat. The internal reference was GAPDH. $^{***}p < 0.001$ vs. Con group. $^{+++}p < 0.001$ vs. LV-NC group. $^{\wedge}p < 0.05$, $^{\wedge\wedge}p < 0.01$, $^{\wedge\wedge\wedge}p < 0.001$ vs. LV-TLR3 group. 8 rats per group, and data from each group were obtained from three repeated experiments. LC3I, microtubule-associated protein 1 light chain 3 I; LC3II, microtubule-associated protein 1 light chain 3 II; P62, sequestosome 1; TLR3, toll-like receptor 3; AMPK, adenosine 5-monophosphate-activated protein kinase; p-AMPK, phosphorylation-AMPK; IRF3, interferon regulatory factor 3; GAPDH, glyceraldehyde-3-phosphate dehydrogenase; Con, control; Mod, model; LV, lentivirus; NC, negative control; CC, compound C; 3-MA, 3-methyladenine.

tory factors IL-1β, IL-6, and IL-18 in the acute liver injury cell model (Fig. 3A–D, $p < 0.001$). However, compared with the LV-TLR3 group, CC or 3-MA abolished the effects of TLR3 on these inflammatory factors (Fig. 3A–D, $p < 0.001$). These results indicated that TLR3 may delay acute liver injury by reducing inflammatory reactions.

Furthermore, to examine the role of TLR3 in cell apoptosis, we assessed cell apoptosis by flow cytometry and western blotting. The results showed that TLR3 overexpression significantly alleviated cell apoptosis in the acute liver injury cell model (Fig. 3E,F, $p < 0.001$). Moreover, compared with the LV-NC group, LV-TLR3 significantly increased Bcl-2 expression and decreased Bax expression (Fig. 3G–I, $p < 0.001$). Similarly, the effects of TLR3 overexpression on cell apoptosis and apoptosis-related proteins were reversed by CC or 3-MA (Fig. 3E–I, $p < 0.05$). These results indicated that TLR3 may delay acute liver injury by inhibiting cell apoptosis.

The Regulatory Effects of TLR3 on Cell Autophagy, Autophagy-Related Proteins, p-AMPK, AMPK and IRF3 Were Reversed by CC and 3-MA

Based on the above results, to investigate whether TLR3 delays acute liver injury by regulating cell autophagy and the AMPK pathway, we detected LC3B and AMPK-related proteins. Interestingly, compared with the LV-NC group, immunofluorescence showed that LV-TLR3 increased LC3B expression (Fig. 4A,B, $p < 0.05$), indicating increased cell autophagy. In addition, autophagy-related proteins (LC3I, LC3II and P62) were also regulated by LV-TLR3. Compared with the LV-NC group, LV-TLR3 increased the LC3II/LC3I value and decreased P62 expression, indicating increased autophagy in the acute liver injury cell model (Fig. 5A–C, $p < 0.001$). However, the effects of LV-TLR3 on cell autophagy were reversed by CC or 3-MA (Fig. 5A–C, $p < 0.001$). These results revealed that TLR3 may delay acute liver injury by increasing cell autophagy in Kupffer cells.

In addition, we evaluated the expression of TLR3, p-AMPK, AMPK and IRF3 proteins in Kupffer cells (Fig. 5D). TLR3 expression was significantly decreased in the Mod group (Fig. 5D,E, $p < 0.001$). Interestingly, compared with the LV-NC group, LV-TLR3 significantly increased IRF3 expression (Fig. 5D,F, $p < 0.001$). This result indicated that the interaction between TLR3 and IRF3 may play a role in alleviating acute liver injury. In particular, compared with LV-NC group, LV-TLR3 significantly increased the p-AMPK/AMPK ratio (Fig. 5D,G, $p < 0.001$). This result revealed that TLR3 may activate the AMPK pathway to delay acute liver injury in Kupffer cells. However, the effects of LV-TLR3 on the p-AMPK/AMPK ratio and IRF3 expression were reversed by CC or 3-MA (Fig. 5D,F,G, $p < 0.05$). Thus, these findings suggest that TLR3 overexpression is associated with increased autophagy and altered AMPK and IRF3 signaling components in Kupffer cells. Pharmacological inhibition of AMPK or autophagy reversed these changes, suggesting that both AMPK and autophagy are associated with the observed TLR3-related effects.

Discussion

As a typical liver injury, LF can occur unpredictably and requires early diagnosis and treatment [31]. Currently, LF remains difficult to treat, and its molecular therapeutic mechanisms are still unclear. In this study, we identified a potential mechanism by which TLR3 delayed GalN/LPS-induced acute liver injury. Our results suggest that TLR3 overexpression is associated with enhanced autophagy and reduced inflammatory responses, potentially involving AMPK phosphorylation and IRF3 upregulation in GalN/LPS-induced acute liver injury.

At the animal level, we established a GalN/LPS-induced acute liver injury model. The increased levels of ALT, AST and LDH in the Mod group indicated that the liver injury model was successfully established. Liver injury is associated with hepatocellular oxidative stress, which contributes to increased serum levels of ALT, AST and LDH. Thus, ALT, AST and LDH levels are associated with oxidative stress and have also been reported to positively correlate with the area of hepatic necrosis [32]. To date, studies exploring the molecular protective mechanisms of TLR3 in acute liver injury remain limited. Our study provides evidence that TLR3 delayed GalN/LPS-induced acute liver injury, an effect associated with enhanced autophagy and regulation of AMPK and IRF3 signaling *in vivo*. TLR3 also alleviated liver tissue lesions and cell apoptosis *in vivo*. Previous studies have shown that autophagy plays a protective role in liver injury [33]. Similarly, up-regulated TLR3 promoted autophagy and reduced myocardial ischemia/reperfusion injury, thereby protecting the myocardium [34], suggesting that TLR3-induced autophagy may exert protective effects in different organs. In our study, TLR3 increased the LC3II/LC3I ratio and decreased P62 expression in the acute liver injury model. Therefore, TLR3 may attenuate acute liver injury by promoting autophagy. In recent years, AMPK has also been shown to be involved in autophagy, and AMPK-associated protective autophagy has been implicated in acute liver injury [35]. More importantly, TLR3 expression was positively correlated with IRF3 expression in hepatocellular carcinoma tissues [36], consistent with our findings. Notably, the effects of TLR3 described above were reversed by CC (an AMPK inhibitor) or 3-MA (an autophagy inhibitor), suggesting that AMPK signaling and autophagy are involved in TLR3-mediated regulation of acute liver injury. Interestingly, inhibition of AMPK signaling or autophagy not only attenuated the downstream protective effects of TLR3 but also altered the expression levels of p-AMPK/AMPK and IRF3. These findings suggest poten-

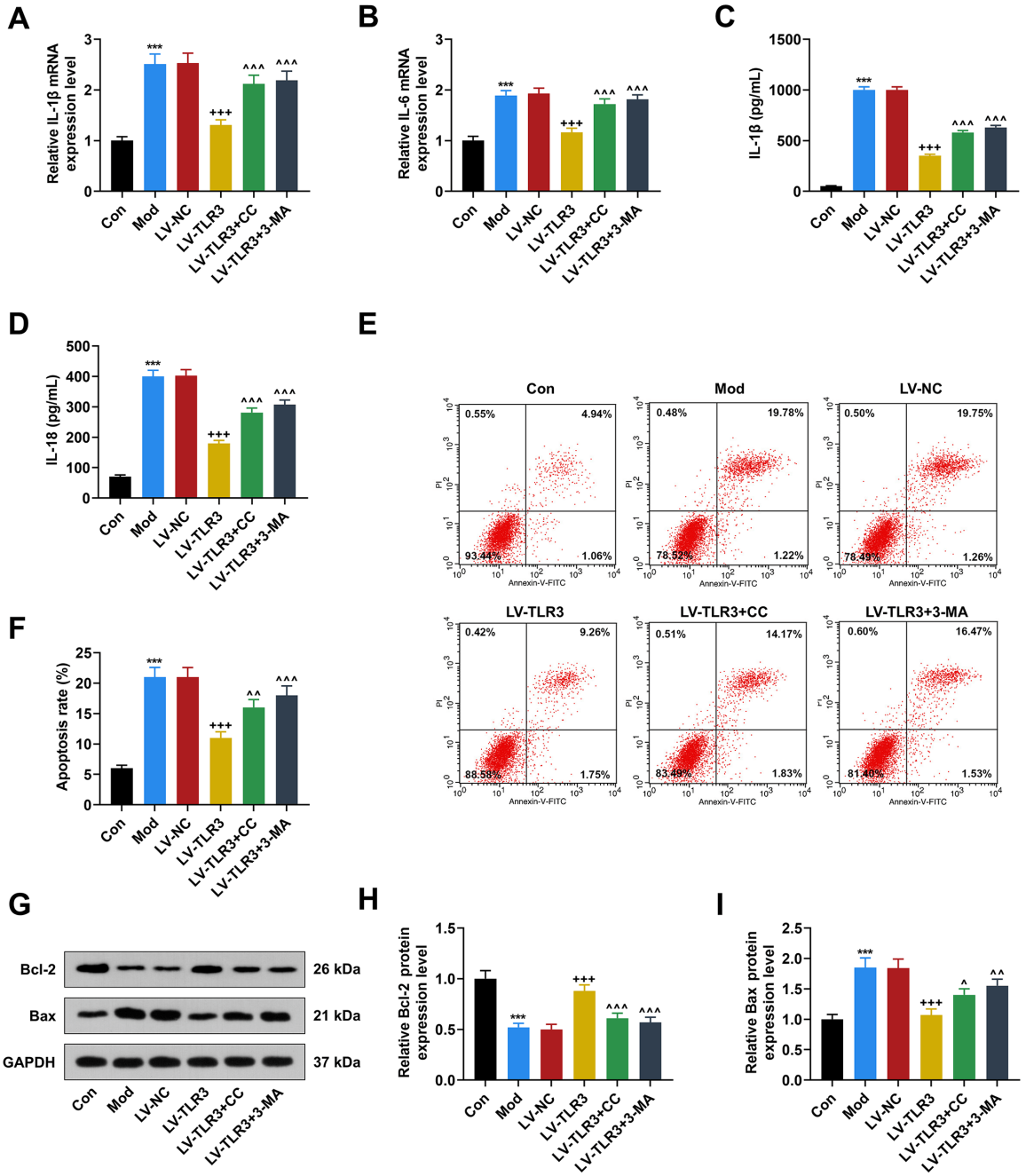

Fig. 3. The regulatory effects of TLR3 on inflammatory factors, cell apoptosis, and apoptosis-related proteins were reversed by CC and 3-MA. For (A–I), Kupffer cells were divided into the following groups: untreated control (Con), model (Mod, GalN/LPS only), lentivirus negative control (LV-NC), TLR3-overexpressing lentivirus (LV-TLR3), LV-TLR3 combined with Compound C (LV-TLR3 + CC), and LV-TLR3 combined with 3-methyladenine (LV-TLR3 + 3-MA) before establishing acute liver injury model. (A,B) qRT-PCR was used to detect the mRNA expression levels of IL-1β and IL-6 in Kupffer cells, with GAPDH as the internal reference. (C,D) ELISA was used to detect the levels of the inflammatory factors IL-1β and IL-18 in Kupffer cells. (E,F) Flow cytometry was used to examine apoptosis in Kupffer cells. (G–I) The protein expression levels of Bcl-2, Bax, and GAPDH n Kupffer cells were detected by western blotting, with GAPDH as the internal reference. $^{***}p < 0.001$ vs. Con group. $^{+++}p < 0.001$ vs. LV-NC group. $^{\wedge}p < 0.05$, $^{\wedge\wedge}p < 0.01$, $^{\wedge\wedge\wedge}p < 0.001$ vs. LV-TLR3 group. Data were obtained from three biologically independent replicates. IL-1β, interleukin-1β; IL-6, interleukin-6; IL-18, interleukin-18; GAPDH, glyceraldehyde-3-phosphate dehydrogenase; Con, control; Mod, model; LV, lentivirus; NC, negative control; TLR3, toll-like receptor 3; CC, compound C; 3-MA, 3-methyladenine; QRT-PCR, quantitative real time polymerase chain reaction; ELISA, enzyme linked immune sorbent assay.

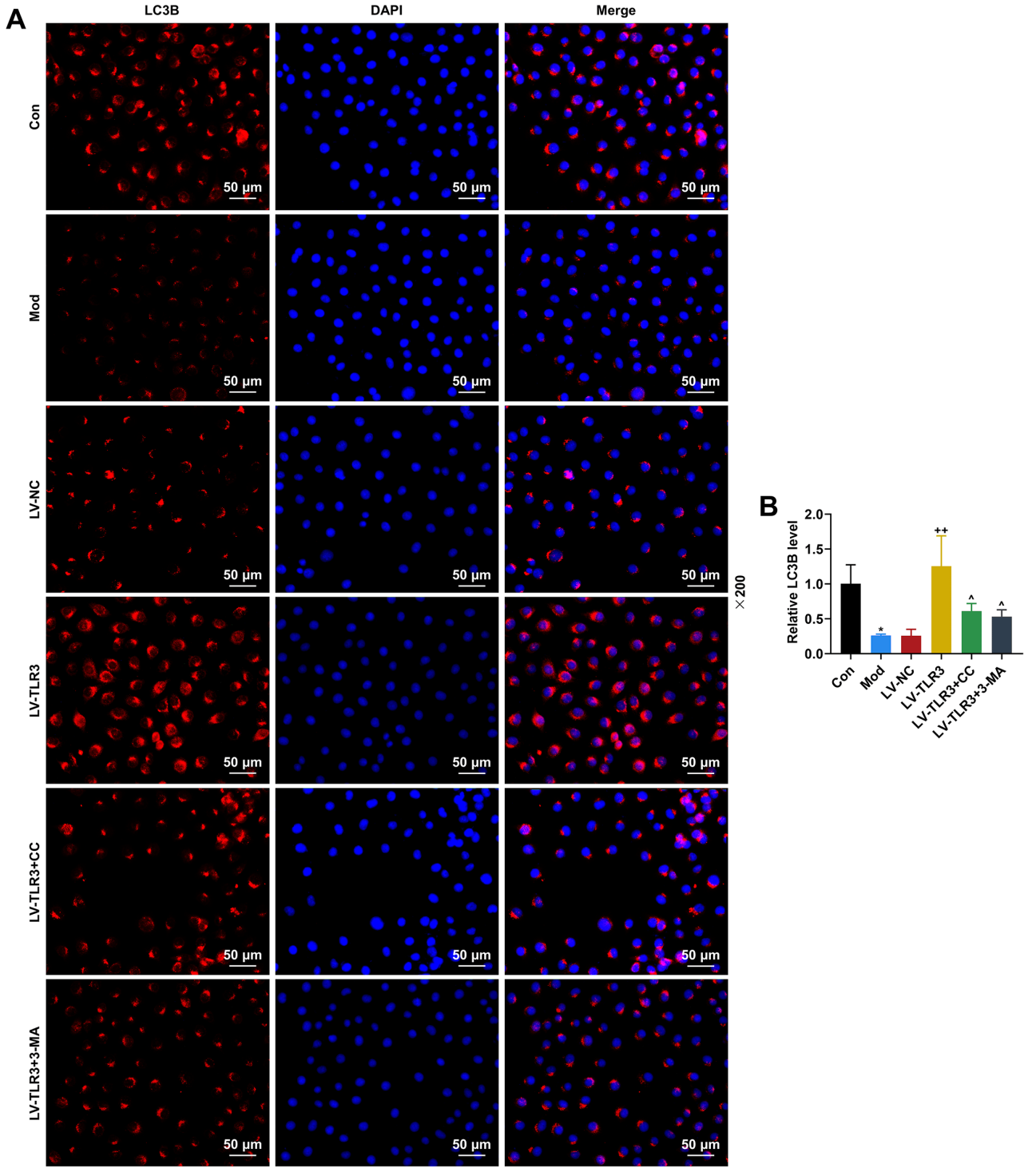

Fig. 4. The TLR3-induced up-regulation of cell autophagy was reversed by CC and 3-MA. (A,B) Kupffer cells were divided into the following groups: untreated control, Mod, LV-NC, LV-TLR3, LV-TLR3 + CC, and LV-TLR3 + 3-MA before establishing acute liver injury model. Immunofluorescence staining was used to detect LC3B expression in Kupffer cells. Positive staining shown in red. Resolution: 50 μm, ×200. Data were obtained from three biologically independent replicates. $^{*}p < 0.05$ vs. Con group. $^{++}p < 0.01$ vs. LV-NC group. $^{\wedge}p < 0.05$ vs. LV-TLR3 group. LC3B, microtubule-associated protein 1 light chain 3 beta; DAPI, 4,6-diamino-2-phenyl indole; Con, control; Mod, model; LV, lentivirus; NC, negative control; TLR3, toll-like receptor 3; CC, compound C; 3-MA, 3-methyladenine.

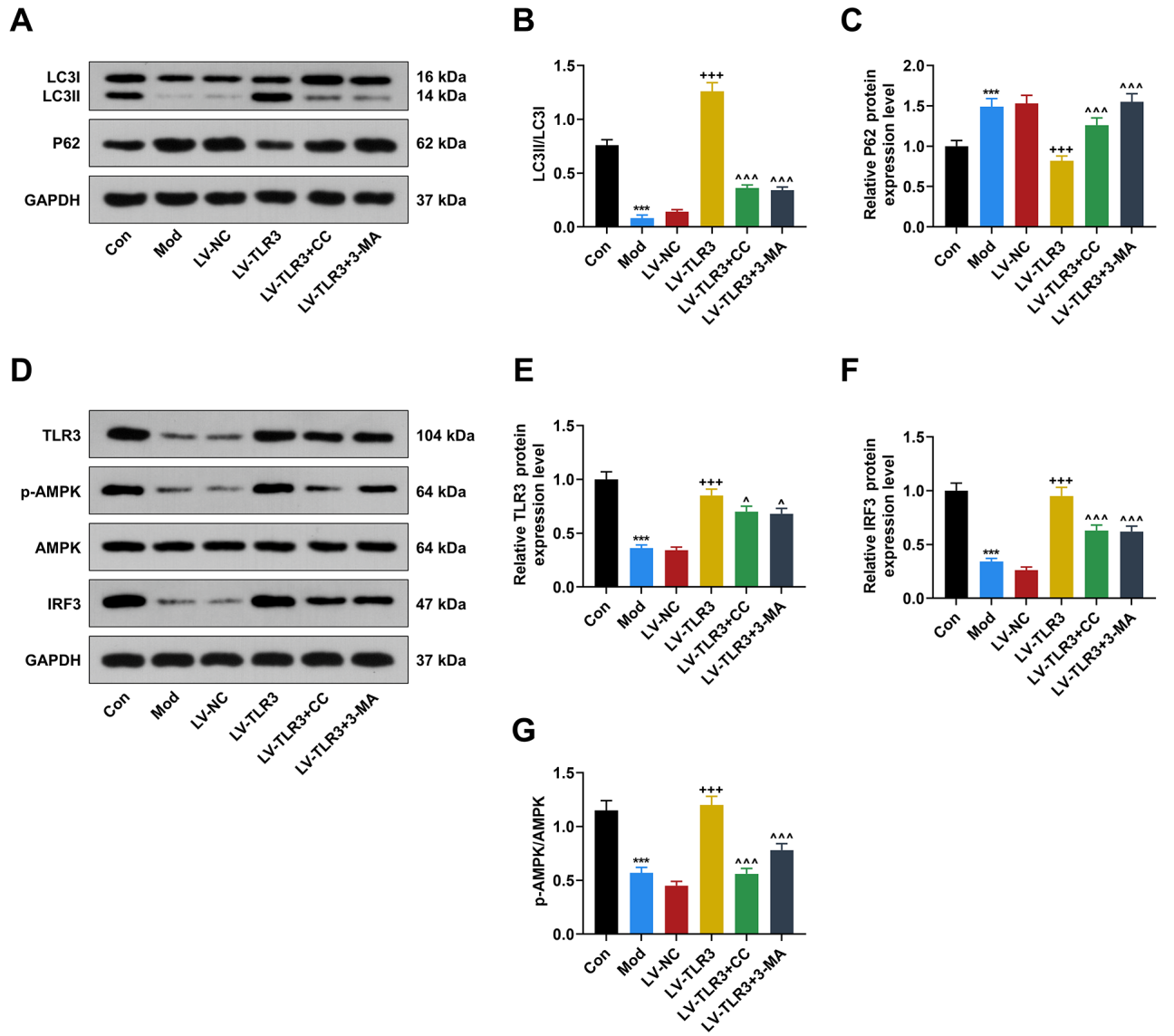

Fig. 5. The regulatory effects of TLR3 on autophagy-related proteins, p-AMPK, AMPK and IRF3 were reversed by CC and 3-MA. For (A–G), Kupffer cells were divided into the following groups: untreated control, Mod, LV-NC, LV-TLR3, LV-TLR3 + CC, and LV-TLR3 + 3-MA, before establishing acute liver injury model. (A–G) The protein expression levels of LC3I, LC3II, P62, TLR3, p-AMPK, AMPK, IRF3 and GAPDH in Kupffer cells were detected by western blotting, with GAPDH as the internal reference. Data were collected from three biologically independent replicates. $^{***}p < 0.001$ vs. Con group. $^{+++}p < 0.001$ vs. LV-NC group. $^{\wedge}p < 0.05$, $^{\wedge\wedge\wedge}p < 0.001$ vs. LV-TLR3 group. LC3I, microtubule-associated protein 1 light chain 3 I; LC3II, microtubule-associated protein 1 light chain 3 II; P62, sequestosome 1; TLR3, toll-like receptor 3; AMPK, adenosine 5-monophosphate-activated protein kinase; p-AMPK, phosphorylation-AMPK; IRF3, interferon regulatory factor 3; GAPDH, glyceraldehyde-3-phosphate dehydrogenase; Con, control; Mod, model; LV, lentivirus; NC, negative control; CC, compound C; 3-MA, 3-methyladenine.

tial feedback regulation or crosstalk among TLR3, AMPK signaling, and autophagy rather than a simple unidirectional regulatory axis. Given that Compound C blocked the effects on both autophagy and IRF3, our pharmacological data are consistent with the involvement of AMPK in the TLR3-associated protective effects. In addition, 3-MA treatment affected AMPK phosphorylation; however, whether this reflects a feedback interaction between autophagy and AMPK signaling requires further investigation using genetic approaches. Previous studies have demonstrated that AMPK is a key regulator of autophagy [37,38]. However, the mechanisms by which autophagy inhibition modulates AMPK signaling remain to be further elucidated.

Likewise, in GalN/LPS-treated Kupffer cells, TLR3 overexpression was associated with reduced inflammatory cytokine expression and cell apoptosis. The *in vitro* data

further support that TLR3 alleviated GalN/LPS-induced acute liver injury by reducing inflammatory factor expression and cell apoptosis, promoting autophagy, and regulating AMPK phosphorylation and IRF3 expression. Kupffer cells play an active role in the response to liver injury. In alcoholic liver disease, TLR3 activation has been shown to inhibit inflammatory responses in Kupffer cells [39], suggesting that TLR3 may alleviate acute liver injury by suppressing inflammation in these cells. Consistently, in our acute liver injury model, TLR3 reduced inflammatory factor expression and alleviated cell apoptosis, indicating that TLR3 exerts anti-inflammatory and anti-apoptotic effects *in vitro*. In addition, AMPK has been reported to inhibit hepatocyte apoptosis in nonalcoholic steatohepatitis by reducing caspase-6 activation [40]. AMPK phosphorylation also promotes autophagy and reduces liver cell apoptosis in non-alcoholic fatty liver disease. Therefore, autophagy and the AMPK pathway may play important roles in liver disorders. Our findings showed that TLR3 promoted autophagy and activated AMPK pathway in Kupffer cells. These data revealed that TLR3 may alleviate acute liver injury by enhancing autophagy and activating the AMPK pathway in Kupffer cells. Moreover, it is well established that TLR3 activation leads to IRF3 phosphorylation and nuclear translocation, thereby regulating type I interferon and inflammatory gene expression [41]. Meanwhile, IRF3 protein can be degraded through the AMPK-related autophagy pathway [42]. In our study, TLR3 overexpression was associated with IRF3 upregulation and reduced inflammatory cytokine expression in Kupffer cells. However, whether the observed IRF3 upregulation reflects direct transcriptional activation or contributes to the reduced inflammatory response in this model remains to be determined. More importantly, the above effects of TLR3 were also reversed by CC or 3-MA in the acute liver injury cell model, consistent with the *in vivo* findings. Therefore, our results provide new insights into the potential role of TLR3 in LF. Together, these findings suggest that TLR3 overexpression is associated with enhanced autophagy and altered AMPK and IRF3 signaling; however, the precise hierarchical relationships among these pathways and their specific roles require further investigation.

There are several limitations to this study. First, although the protective effects of TLR3 in acute liver injury were associated with regulation of AMPK signaling and IRF3 expression in both *in vivo* and *in vitro* experiments, the precise regulatory mechanisms, particularly whether TLR3 acts upstream of AMPK or whether autophagy reciprocally modulates AMPK and IRF3, has not been fully elucidated and requires further investigation using genetic approaches. Additionally, Kupffer cells were used as the *in vitro* model in this study. Although Kupffer cells are primary targets of LPS stimulation, and investigating TLR3 regulation in these cells is mechanistically relevant to understanding how innate immune modulation affects acute liver injury, findings from Kupffer cells cannot fully represent hepatocyte injury. Future studies should establish hepatocyte injury models to further strengthen the reliability of these conclusions. Finally, these findings were obtained from experimental models, and their translational relevance to human liver failure requires further validation using clinical samples and studies.

Conclusion

In summary, this study demonstrates that TLR3 overexpression is associated with attenuated GalN/LPS-induced acute liver injury, accompanied by enhanced autophagy, increased AMPK phosphorylation, and IRF3 upregulation. Our findings suggest that TLR3 may represent a potential protective target for acute liver injury. Further studies are needed to clarify the precise molecular interactions involved and to validate these findings in clinical settings.

Availability of Data and Materials

The datasets used or analyzed during the current study are available from the corresponding author upon reasonable request.

Author Contributions

YZ and JZ designed the research study; YZ, JZ and XC performed the research; YZ, JZ and XC collected and analyzed the data. YZ and JZ have been involved in drafting the manuscript and all authors have been involved in revising it critically for important intellectual content. All authors gave final approval of the version to be published. All authors have participated sufficiently in the work to take public responsibility for appropriate portions of the content and agreed to be accountable for all aspects of the work in ensuring that questions related to its accuracy or integrity.

Ethics Approval and Consent to Participate

All animal experiments were approved by the Institutional Animal Care and Use Committee of the Zhejiang Center of Laboratory Animals (Approval No. ZJCLA-IACUC-20011191) and were conducted in accordance with the China Council on Animal Care and Use guidelines. This study adhered to the ARRIVE (Animal Research: Reporting of *In Vivo* Experiments) guidelines 2.0 for reporting *in vivo* experiments.

Acknowledgment

Not applicable.

Funding

This research received no external funding.

Conflict of Interest

The authors declare no conflict of interest.

Supplementary Material

Supplementary material associated with this article can be found, in the online version, at https://doi.org/10.24976/Discov.Med.202638212.234.

References

[1] Kabbani AR, Tergast TL, Manns MP, Maasoumy B. Treatment strategies for acute-on-chronic liver failure. Medizinische Klinik, Intensivmedizin Und Notfallmedizin. 2021; 116: 3–16. https://doi.org/10.1007/s00063-019-00613-x

[2] Maiwall R, Kulkarni AV, Arab JP, Piano S. Acute liver failure. Lancet (London, England). 2024; 404: 789–802. https://doi.org/10.1016/S0140-6736(24)00693-7

[3] Wong F, Piano S, Singh V, Bartoletti M, Maiwall R, Alessandria C, et al. Clinical features and evolution of bacterial infection-related acute-on-chronic liver failure. Journal of Hepatology. 2021; 74: 330–339. https://doi.org/10.1016/j.jhep.2020.07.046

[4] Bernal W, Karvellas C, Saliba F, Saner FH, Meersseman P. Intensive care management of acute-on-chronic liver failure. Journal of Hepatology. 2021; 75 Suppl 1: S163–S177. https://doi.org/10.1016/j.jhep.2020.10.024

[5] Larsen FS, Saliba F. Liver support systems and liver transplantation in acute liver failure. Liver International: Official Journal of the International Association for the Study of the Liver. 2025; 45: e15633. https://doi.org/10.1111/liv.15633

[6] Khalil A, Quaglia A, Gélat P, Saffari N, Rashidi H, Davidson B. New Developments and Challenges in Liver Transplantation. Journal of Clinical Medicine. 2023; 12: 5586. https://doi.org/10.3390/jcm12175586

[7] Liu J, Wu Y, Meng S, Xu P, Li S, Li Y, et al. Selective autophagy in cancer: mechanisms, therapeutic implications, and future perspectives. Molecular Cancer. 2024; 23: 22. https://doi.org/10.1186/s12943-024-01934-y

[8] Chen X, Su Q, Gong R, Ling X, Xu R, Feng Q, et al. LC3-associated phagocytosis and human diseases: Insights from mechanisms to therapeutic potential. FASEB Journal: Official Publication of the Federation of American Societies for Experimental Biology. 2024; 38: e70130. https://doi.org/10.1096/fj.202402126R

[9] Zhang C, Liu X, Liu X, Hua R, Liu H, Ma J, et al. Adenosine kinase protects against acetaminophen-induced acute liver injury by activating autophagy in hepatocytes. Cell Biology and Toxicology. 2024; 40: 59. https://doi.org/10.1007/s10565-024-09906-0

[10] Arab HH, Eid AH, Alsufyani SE, Ashour AM, Alnefaie AM, Alsharif NM, et al. Activation of AMPK/mTOR-Driven Autophagy and Suppression of the HMGB1/TLR4 Pathway with Pentoxifylline Attenuates Doxorubicin-Induced Hepatic Injury in Rats. Pharmaceuticals (Basel, Switzerland). 2024; 17: 681. https://doi.org/10.3390/ph17060681

[11] Tseng DY, Wang ST, Ballantyne R, Liu CH. Adenosine 5'-monophosphate-activated protein kinase (AMPK) negatively regulates the immunity and resistance to Vibrio alginolyticus of white shrimp, Penaeus vannamei. Fish & Shellfish Immunology. 2023; 139: 108884. https://doi.org/10.1016/j.fsi.2023.108884

[12] Liu Z, Jin Q, Yin J. Pachymic Acid A Alleviates Myocardial Injury in Acute Myocardial Infarction Mice by Regulating the AMPK/mTOR Pathway-Mediated Autophagy. Discovery Medicine. 2025; 37: 1630–1638. https://doi.org/10.24976/Discov.Med.202537199.142

[13] Lu X, Xuan W, Li J, Yao H, Huang C, Li J. AMPK protects against alcohol-induced liver injury through UQCRC2 to up-regulate mitophagy. Autophagy. 2021; 17: 3622–3643. https://doi.org/10.1080/15548627.2021.1886829

[14] Wang Q, Wei S, Zhou S, Qiu J, Shi C, Liu R, et al. Hyperglycemia aggravates acute liver injury by promoting liver-resident macrophage NLRP3 inflammasome activation via the inhibition of AMPK/mTOR-mediated autophagy induction. Immunology and Cell Biology. 2020; 98: 54–66. https://doi.org/10.1111/imcb.12297

[15] Yu Q, Zou L, Yuan X, Fang F, Xu F. Dexmedetomidine Protects Against Septic Liver Injury by Enhancing Autophagy Through Activation of the AMPK/SIRT1 Signaling Pathway. Frontiers in Pharmacology. 2021; 12: 658677. https://doi.org/10.3389/fphar.2021.658677

[16] Han B, Zhang C, Wang X, Song H, Zhang L, Li T, et al. The Functional Mechanisms of Toll-Like Receptor 3 and Its Implications in Digestive System Tumors. Frontiers in Bioscience (Landmark Edition). 2023; 28: 297. https://doi.org/10.31083/j.fbl2811297

[17] Chen Y, Lin J, Zhao Y, Ma X, Yi H. Toll-like receptor 3 (TLR3) regulation mechanisms and roles in antiviral innate immune responses. Journal of Zhejiang University. Science. B. 2021; 22: 609–632. https://doi.org/10.1631/jzus.B2000808

[18] Zhuge A, Li B, Yuan Y, Lv L, Li Y, Wu J, et al. Lactobacillus salivarius LI01 encapsulated in alginate-pectin microgels ameliorates D-galactosamine-induced acute liver injury in rats. Applied Microbiology and Biotechnology. 2020; 104: 7437–7455. https://doi.org/10.1007/s00253-020-10749-y

[19] Zhang G, Li R, Li W, Yang S, Sun Q, Yin H, et al. Toll-like receptor 3 ablation prevented high-fat diet-induced obesity and metabolic disorder. The Journal of Nutritional Biochemistry. 2021; 95: 108761. https://doi.org/10.1016/j.jnutbio.2021.108761

[20] Qin C, Niu C, Shen Z, Zhang Y, Liu G, Hou C, et al. RACK1 T50 Phosphorylation by AMPK Potentiates Its Binding with IRF3/7 and Inhibition of Type 1 IFN Production. Journal of Immunology (Baltimore, Md.: 1950). 2021; 207: 1411–1418. https://doi.org/10.4049/jimmunol.2100086

[21] Song Y, Zhang Z, Yu Z, Xia G, Wang Y, Wang L, et al. Wip1 Aggravates the Cerulein-Induced Cell Autophagy and Inflammatory Injury by Targeting STING/TBK1/IRF3 in Acute Pancreatitis. Inflammation. 2021; 44: 1175–1183. https://doi.org/10.1007/s10753-021-01412-3

[22] Hu L, Gao D, Lv H, Lian L, Wang M, Wang Y, et al. Finding New Targets for the Treatment of Heart Failure: Endoplasmic Reticulum Stress and Autophagy. Journal of Cardiovascular Translational Research. 2023; 16: 1349–1356. https://doi.org/10.1007/s12265-023-10410-9

[23] Wu Y, Jin S, Liu Q, Zhang Y, Ma L, Zhao Z, et al. Selective autophagy controls the stability of transcription factor IRF3 to balance type I interferon production and immune suppression. Autophagy. 2021; 17: 1379–1392. https://doi.org/10.1080/15548627.2020.1761653

[24] Wang Q, Liu L, Zhang S, Ming Y, Liu S, Cheng K, et al. Long noncoding RNA NEAT1 suppresses hepatocyte proliferation in fulminant hepatic failure through increased recruitment of EZH2 to the LATS2 promoter region and promotion of H3K27me3 methylation. Experimental & Molecular Medicine. 2020; 52: 461–472. https://doi.org/10.1038/s12276-020-0387-z

[25] Mohamed DZ, El-Sisi AEDES, Sokar SS, Shebl AM, Abu-Risha SES. Targeting autophagy to modulate hepatic ischemia/reperfusion injury: A comparative study between octreotide and melatonin as autophagy modulators through AMPK/PI3K/AKT/mTOR/ULK1 and Keap1/Nrf2 signaling

pathways in rats. European Journal of Pharmacology. 2021; 897: 173920. https://doi.org/10.1016/j.ejphar.2021.173920

[26] Wang Y, Wang JL, Ma HC, Tang ZT, Ding HR, Shi XL. Mesenchymal stem cells increase heme oxygenase 1-activated autophagy in treatment of acute liver failure. Biochemical and Biophysical Research Communications. 2019; 508: 682–689. https://doi.org/10.1016/j.bbrc.2018.11.146

[27] Wang K, Lv L, Yan R, Wang Q, Jiang H, Wu W, et al. Bifidobacterium longum R0175 Protects Rats against d-Galactosamine-Induced Acute Liver Failure. MSphere. 2020; 5: e00791–19. https://doi.org/10.1128/mSphere.00791-19

[28] Jiang H, Yan R, Wang K, Wang Q, Chen X, Chen L, et al. Lactobacillus reuteri DSM 17938 alleviates d-galactosamine-induced liver failure in rats. Biomedicine & Pharmacotherapy = Biomedecine & Pharmacotherapie. 2021; 133: 111000. https://doi.org/10.1016/j.biopha.2020.111000

[29] Zhang X, Zhang L, Bi Y, Xi T, Zhang Z, Huang Y, et al. Inhibition of autophagy by 3-methyladenine restricts murine cytomegalovirus replication. Journal of Medical Virology. 2021; 93: 5001–5016. https://doi.org/10.1002/jmv.26787

[30] Liu Y, He H, Fan L, Yuan J, Huang H, Yang W, et al. Compound C attenuates NLRP3 inflammasome despite AMPK knockdown in LPS plus palmitate-induced THP-1 cells. Naunyn-Schmiedeberg's Archives of Pharmacology. 2020; 393: 67–76. https://doi.org/10.1007/s00210-019-01712-4

[31] Stravitz RT, Fontana RJ, Karvellas C, Durkalski V, McGuire B, Rule JA, et al. Future directions in acute liver failure. Hepatology (Baltimore, Md.). 2023; 78: 1266–1289. https://doi.org/10.1097/HEP.0000000000000458

[32] Zhou Y, Fan X, Jiao T, Li W, Chen P, Jiang Y, et al. SIRT6 as a key event linking P53 and NRF2 counteracts APAP-induced hepatotoxicity through inhibiting oxidative stress and promoting hepatocyte proliferation. Acta Pharmaceutica Sinica. B. 2021; 11: 89–99. https://doi.org/10.1016/j.apsb.2020.06.016

[33] Salete-Granado D, Carbonell C, Puertas-Miranda D, Vega-Rodríguez VJ, García-Macia M, Herrero AB, et al. Autophagy, Oxidative Stress, and Alcoholic Liver Disease: A Systematic Review and Potential Clinical Applications. Antioxidants (Basel, Switzerland). 2023; 12: 1425. https://doi.org/10.3390/antiox12071425

[34] Chen E, Chang H, Gao R, Qiu Y, Chen H, Cheng X, et al. Poly(I:C) attenuates myocardial ischemia/reperfusion injury by restoring autophagic function. FASEB Journal: Official Publication of the Federation of American Societies for Experimental Biology. 2022; 36: e22317. https://doi.org/10.1096/fj.202101220RR

[35] Wu J, Zhou F, Fan G, Liu J, Wang Y, Xue X, et al. Ferulic acid ameliorates acetaminophen-induced acute liver injury by promoting AMPK-mediated protective autophagy. IUBMB Life. 2022; 74: 880–895. https://doi.org/10.1002/iub.2625

[36] Zhang C, Liu S, Yang M. The Role of Interferon Regulatory Factors in Non-Alcoholic Fatty Liver Disease and Non-Alcoholic Steatohepatitis. Gastroenterology Insights. 2022; 13: 148–161. https://doi.org/10.3390/gastroent13020016

[37] Mihaylova MM, Shaw RJ. The AMPK signalling pathway coordinates cell growth, autophagy and metabolism. Nature Cell Biology. 2011; 13: 1016–1023. https://doi.org/10.1038/ncb2329

[38] Park JM, Lee DH, Kim DH. Redefining the role of AMPK in autophagy and the energy stress response. Nature Communications. 2023; 14: 2994. https://doi.org/10.1038/s41467-023-38401-z

[39] Zhang ZH, Yang HX, Yang JL, Jiang XL, Wang SQ, Wu YL, et al. TLR3-mediated NET formation and macrophage activation in acute liver failure: Targeting IL-36 signaling to attenuate inflammatory drivers. International Immunopharmacology. 2025; 161: 115112. https://doi.org/10.1016/j.intimp.2025.115112

[40] Banerjee A, Das D, Maji BK. Non-alcoholic Steatohepatitis and Hepatocellular Carcinoma are Influenced by Oxidative Stress, Inflammation, and Apoptosis via Activating the AMPKCaspase Axis and JAK/STAT Pathway. Journal of Comprehensive Health. 2024; 12: 12–15.

[41] He S, Liao Z, Tang D, Zeng Z, Wang B, Zhou P, et al. Regulation of type I interferon factor secretion via the TLR3 signaling pathway after PRV infection of mouse trigeminal ganglion cells. Virus Genes. 2025; 61: 574–587. https://doi.org/10.1007/s11262-025-02146-2

[42] Chakravarty S, Fan S, Chakravarti R, Chattopadhyay S. Autophagic checks and balances of cellular immune responses. Autophagy Reports. 2022; 1: 83–87. https://doi.org/10.1080/27694127.2022.2058677